Journal of Hazardous Materials 371 (2019) 115–122

Contents lists available at ScienceDirect

Journal of Hazardous Materials

journal homepage: www.elsevier.com/locate/jhazmat

Sequential photocatalysis and biological treatment for the enhanced degradation of the persistent azo dye methyl red

Tatoba R. Waghmode[a,b], Mayur B. Kurade[c], Ramchandra T. Sapkal[d], Chandrakant H. Bhosale[d], Byong-Hun Jeon[c,*], Sanjay P. Govindwar[a,c,*]

[a] Department of Biochemistry, Shivaji University, Kolhapur, 416004, India
[b] Institute of Genetics and Developmental Biology, Chinese Academy of Sciences, Shijiazhuang, China
[c] Department of Earth Resources and Environmental Engineering, Hanyang University, Seoul, 04763, South Korea
[d] Department of Physics, Shivaji University, Kolhapur, 410006, India

GRAPHICAL ABSTRACT

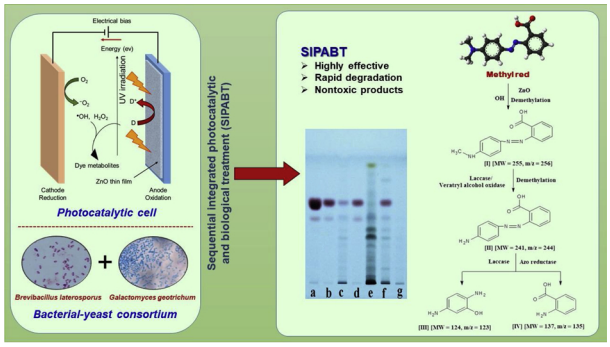

ARTICLE INFO

Keywords:
Photocatalysis
Microbial consortium
Decolorization
Degradation
Integrated treatment

ABSTRACT

A combination of photocatalysis and biodegradation is a promising approach for the removal of xenobiotic organic compounds from wastewater, since photocatalysis cleaves the molecules into simpler intermediates that are later mineralized by microorganisms. Sequential photocatalytic and biological treatment (SPABT) consisting of ZnO as a photocatalyst and a microbial consortium (*Galactomyces geotrichum* and *Brevibaccilus laterosporus*) enhanced the degradation of a model textile dye, methyl red (MR). SPABT completely decolorized 500 mg MR/L within 4 h. Biotreatment alone required 6 h for 100% decolorization. A maximum of 70% decolorization was achieved with the photocatalytic treatment but reductions in COD and toxicity were not adequate. Significant elevated activities of enzymes, including azo reductase, laccase and veratryl alcohol oxidase, were observed in the microbial consortium after exposure of MR. The degradation pathway and products of MR varied with treatment applied. The persistent azo bond was cleaved by following photocatalytic treatment with the microbial biotreatment. Tests with *Sorghum vulgare* and *Phaseolus mungo* indicated the products obtained by SPABT were non-phytotoxic.

* Corresponding authors at: Department of Earth Resources and Environmental Engineering, Hanyang University, Seoul, 04763, South Korea.
E-mail addresses: bhjeon@hanyang.ac.kr (B.-H. Jeon), spgovindwar@hanyang.ac.kr (S.P. Govindwar).

https://doi.org/10.1016/j.jhazmat.2019.03.004
Received 26 July 2018; Received in revised form 27 February 2019; Accepted 1 March 2019
Available online 01 March 2019
0304-3894/

1. Introduction

Twenty percent of the world population has difficulty in accessing potable water and 40% suffer from improper hygiene because of their water resources are contaminated with harmful anthropogenic and naturally occurring compounds [1,2]. Over 7×10^5 tons of synthetic dyes are annually produced worldwide, of which around 15% of the dyes are released into the environment by various dyeing industries [3]. Textile industry effluent containing dyes causes severe environmental pollution even at low concentrations that affects transparency and creates aesthetic problems [4]. Hence, effective treatment of textile effluent before discharge in to the environment is mandatory.

Among advanced oxidation processes (AOPs), photocatalysis using semiconductors viz., TiO_2 and ZnO, appears effective for textile wastewater treatment [5]. Photocatalytic conversion using ZnO showed better degradation efficiency than TiO_2 for removing organic compounds from water [6,7]. AOPs are often effective and efficient, but may not be feasible due to cost, incomplete mineralization, and toxicity of some of the diverse products. In contrast, biological methods including bacteria, fungi and plants are effectively being used for textile dye degradation [8–11]. The use of microbial consortia enhances dye degradation due to the wide range of enzymes activated in a mixed culture. The downside of this process is the requirement of long retention times for the transformation of an active molecule and its complete mineralization.

Combining AOP and biodegradation can be a viable approach for degrading xenobiotics in wastewater [12–15]. Photocatalysis is based on the formation of free radicals using UV irradiation in combination with semiconductor ZnO particles [16], and biological system relies on enzymatic machineries involving oxidoreductive enzymes. In a sequential scheme, photocatalytic process can breakdown the complex molecular structures by free radical attack, generating products that are more readily biodegradable [17]. However, photocatalytic processes can over oxidize organic compounds and generate toxic products [14,15]. Thus, it is important to restrict a sequential integrated process before over-oxidation of organic compounds. To avoid such issues, researchers have tried coupling of these techniques in the same reactor. However, this approach has technical difficulties such as loss of microbial biomass from UV exposure and requires costly microporous carriers to protect the microbes from UV light [16–18]. In contrast, a single and a sequential combination process would simplify flow and offer an effective treatment unless the primary photocatalytic component must be restricted to a limited period. While studying feasibility of photocatalysis and a biological treatment for the removal of azo dyes from aqueous effluents, Chebli et al. [19] achieved limited success enhancing mineralization of orange II among acid red 183, biebrich scarlet, and methyl red.

Here we evaluate a sequential photocatalytic and biological treatment to remove methyl red (MR) from water. A photocatalyst, ZnO and microbial consortium consisting of a yeast, *Galactomyces geotrichum* and a bacterium, *Brevibaccilus laterosporus* was sequentially employed for the enhanced degradation of MR. The coupling of these two treatments were preferred because of increased biodegradability by photocatalytic treatment and breakage of azo bond due to biological treatment. We have also studied the possible degradation pathways considering oxidation by free radicals, enzymes induced, and conducted FTIR and GC-MS analysis. The toxicity of the products generated after the degradation of MR was also evaluated to confirm the effectiveness of the SPABT.

2. Materials and methods

2.1. Chemicals, microbiome used and culture conditions

Methyl red (MR) was obtained from textile industry located at Ichalkaranji, India. Yeast extract, peptone, malt extract, veratryl alcohol and l-catechol were obtained from Hi Media, Mumbai, India. All other chemicals were acquired from SRL, India. High purity and analytical grade chemicals were used for this study. *Brevibaccilus laterosporus* MTCC 2298 and *Galactomyces geotrichum* MTCC 1360 were acquired from Microbial Type Culture Collection, India. *G. geotrichum* was maintained on agar slants of medium containing peptone, yeast extract, malt extract, and glucose (5, 3, 3, 10 g/L, respectively). and *B. laterosporus* on nutrient agar slants of the medium containing beef extract, yeast extract, bacteriological peptone, and NaCl (1, 2, 10, 5 g/L, respectively).

2.2. Preparation of GB consortium

The consortium was selected based on our previous work [20]. Briefly, 1 g of wet mycelia of *G. geotrichum* (24 h grown in yeast culture medium, at 30 °C) was washed several times with sterile distilled water. This cell suspension was mixed with *B. laterosporus* (9×10^7 cells/mL) pre-grown in nutrient broth at 30 °C.

2.3. ZnO thin film synthesis for photocatalysis

ZnO films were prepared on transparent conducting glass of fluorine doped tin oxide (FTO) (TCO22-15, 15 Ω/cm^2 Solaronix, Switzerland) using spray pyrolytic deposition method [7]. Zinc acetate (0.2 M in methanol and water) was sprayed onto FTO substrates at 400 °C using a pneumatic glass nozzle. The compressed air was used as a carrier gas. The structural properties of the ZnO thin film were determined with Cu-K_α (1.5405 A°) radiation in the span of 20 to 80° using X-ray diffractometer (Philips, PW-1710). Scanning Electron Microscope (SEM, JEOL JSM-6360) was used to observe surface morphology. Optical absorption was measured with spectrometer (Systronic-119) in a range of 200–1100 nm.

2.4. Decolorization and chemical oxygen demand

Degradation of MR using photocatalytic-ZnO and biological treatment with GB consortium was performed using 100 mL dye solution (500 mg/L) in 250 mL Erlenmeyer flask at different experimental conditions (Table 1). For the photocatalytic ZnO treatment, MR solution (500 mg/L) was recirculated in photocatalytic reactor under UVA illumination for 2 h at 30 °C, pH 7.0. For the GB consortium treatment, 50 mg dye was added to 100 mL of growth medium containing 9×10^7 cells/mL of *G. geotrichum* and *B. laterosporus*. The flask was incubated at 30 °C and pH 7.0 for 2 h with shaking at 120 rpm. Flasks were sampled (4 mL) at 30-min intervals during the incubation. Suspended particles were removed by centrifugation (5000 ×g, 20 min). All spectrophotometric measurements were made at pH 7, adjusting the pH with 0.01 M NaOH or HCl [21]. The yellow color of methyl red was quantified at 420 nm using Hitachi UV–vis spectrophotometer (U 2800, Japan) [22]. COD was measured as per the standard method (APHA, 1998 method 5220-B). All experiments were conducted in triplicate.

2.5. Sequential treatments

Photocatalytic-ZnO and biological treatments were coupled for MR decolorization. In separate experiments (Table 1), decolorization of MR was carried out by a) initial photocatalytic-ZnO (2 h) followed by biological treatment (2 h) (SPABT), and b) initial biological treatment (2 h) followed by photocatalytic-ZnO (2 h) (SBAPT) (Table 1). Photocatalytic-ZnO system was conducted at 30 °C, pH 7.0 for 2 h, and biological treatment (GB consortium) using nutrient medium at 30 °C, pH 7.0 for 2 h with shaking (120 rpm). For the SBAPT, the microbial cells from the first phase of treatment were separated from the effluent by centrifuging at 5000 × g for 5 min, and the supernatant was introduced into photocatalytic-ZnO system.

Table 1
Treatment descriptions, process flow, and decolorization efficiency for methyl red (500 mg/L).

Treatment code	Process flow and description of the treatment				Total treatment time (h)	Decolorization (%)	COD reduction (%)
	Phase 1 Treatment	Time (h)	Phase 2 Treatment	Time (h)			
SPHOT	Photocatalysis-ZnO	2	NA	—	2	33	6
SPHOT	Photocatalysis-ZnO	6	NA	—	6	70	16
SBIOT	Biological treatment[#]	2	NA	—	2	64	31
SBIOT	Biological treatment[#]	6	NA	—	6	100	70
SBAPT	Biological treatment[#]	2	Photocatalysis-ZnO	2	4	78	45
SPABT[†]	Photocatalysis-ZnO	2	Biological treatment[#]	2	4	100	80

NA: Not applicable.
SPHOT: Single photocatalytic treatment.
SBIOT: Single biological treatment with GB consortium.
SBAPT: Sequential biological treatment and photocatalytic treatment.
SPABT: Sequential photocatalytic and biological treatment.
[†] Among all verified treatments, this process (SPABT) showed the enhanced decolorization.
[#] Biological treatment contained GB consortium (G- *Galactomyces geotrichum*, B-*Brevibacillus laterosporus*).

2.6. Cell free extract for the determination of enzymatic activities

The GB consortium was prepared as above and biomass recovered by centrifugation (10,000 x g, 25 min). The biomass was added to potassium phosphate buffer (50 mM, pH 7.4), sonicated (Sonics-vibracell ultrasonic processor, USA) [20] and centrifuged (10,000 × g, 25 min) at 4 °C. The obtained supernatant was used as a source of intracellular enzymes involved in dye degradation.

Activities of the oxidative enzymes were determined spectrophotometrically (Hitachi U 2800, Japan) at 25 °C. Laccase activity was assessed in 2 mL assay mixture containing 3′,3′-diaminobenzidine tetrahydrate (5 mM) in acetate buffer (0.1 M, pH 4.8) and absorbance measured at 410 nm [20]. Veratryl alcohol oxidase activity was estimated in an assay mixture (2 mL: citrate phosphate buffer (0.1 M, pH 3.0), veratryl alcohol (1 mM), and 0.2 mL enzyme). Veratraldehyde formation was measured at 310 nm. Activity of tyrosinase was determined as described in our earlier work [20].

NADH-DCIP reductase activity was measured at 590 nm by adding 250 μM NADH in 2.0 mL of assay mixture containing 50 mM potassium phosphate buffer (pH 7.4), 25 μM DCIP and 0.04 mL cell-free supernatant [22]. Decrease in NADPH concentration in a reaction mixture (2 ml: Tris-HCl (100 mM, pH 7.4), NADPH (25 μM) and riboflavin (10 μM)) was measured at 340 nm to determine the riboflavin reductase activity, using 0.0063 μM^{-1} cm^{-1}as a molar extinction coefficient. Azo reductase activity was assayed in a 2 mL assay mixture (Potassium phosphate buffer (50 mM, pH 7.4), MR (25 μM), and NADH (50 μM)). The reaction was initiated by adding cell-free supernatant (0.2 mL) and monitored at 430 nm [19]. An extinction coefficient 0.023 μM^{-1} cm^{-1} was used to determine the concentration of reduced MR. The enzyme activity was expressed in units (amount of enzyme required to reduce 1 μM of MR min^{-1} mg^{-1} protein). All assays were conducted in triplicate.

2.7. Analysis of treatment products

The products of all treatments were extracted from solution with ethyl acetate (v/v) and dehydrated with anhydrous Na_2SO_4. Ten-microliter samples of the control (MR without treatment) and the extracted MR products dissolved in methanol were spotted on Lichrospher Silica gel 60 $F_{254}S$ plates to analyze using HPTLC (CAMAG, Switzerland). After running, the plates were developed in saturated (for 20 min) twin trough chamber (10 × 10 cm) with ethyl acetate: methanol (3:7, v/v, 10 mL). The developed HPTLC plates were monitored at 254 nm in UV chamber. WinCATS 1.4.4.6337 software was used for analysis of results.

The products were also analyzed by HPLC (Waters model no. 2690). Briefly, 10 μL of 0.2 μm membrane filtered supernatant was injected in a C_{18} column (4.6 mm × 250 mm, symmetry). HPLC was performed isocratically with methanol at a flow rate of 1 mL min^{-1} for 10 min. Eluted compounds were detected at 530 and 280 nm using dual detector.

Extracted products (KBr pellets; 5:95, w/w) were analyzed for functional group changes using Fourier transform infrared spectroscopy (8400S Shimadzu, Japan) in the 400-4000 cm^{-1} region. Formed products of MR were also identified using a gas chromatography with mass spectroscopy (GC–MS) (QP2010 Shimadzu, Japan). A Restek capillary column (0.25 mm, 60 m; XTI™-5) was used; initial temperature was 80 °C for 2 min, increased 10 °C/min to 280 °C, and held for 7 min. Helium was the carrier gas (1.0 mL/min). Temperatures of the injection port and GC–MS interface were maintained at 280 °C and 290 °C, respectively. Ionization voltage was 70 eV. The products were identified by fragmentation patterns and mass spectra using the NIST spectral library.

2.8. Phytotoxicity of products

Sorghum vulgare and *Phaseolus mungo* (agricultural plants) were used to evaluate the phytotoxicity of original dye and generated products. Ten seeds were placed in Petri dishes containing sand and watered with tap water (control), MR (2000 mg/L), and SPABT-generated MR transformation products. Petri plates were kept at room temperature. Shoot and root length and percent germination were measured at 7 d.

2.9. Statistical analysis

Three independent sets of experiments were conducted. Data were examined using a one-way analysis of variance at $p \leq 0.05$ and the Tukey-Kramer multiple comparison test.

3. Results and discussion

3.1. Decolorization and COD determination

Decolorization by SPHOT and SBIOT was 33 and 64%, respectively, with a 6 and 31% reduction in chemical oxygen demand (COD) within 2 h. The respective treatments further increased decolorization to 70 and 100% with 16 and 70% reduction in COD when the process was prolonged to 6 h. Photocatalytic process break down complex molecular structures through free radical attack (hydroxyl radical ($^{\cdot}OH$), superoxide anions ($O_2^{\cdot-}$) and hydrogen peroxide (H_2O_2)) and generates readily biodegradable products [17]. As indicated in our earlier study [7], the synthesized thin films were densely hexagonal crystal structure

with lateral (002) plane growth and covered the film surface homogeneously (Fig. S1a). Optical transmission spectra of the ZnO thin film showed uniformity and transparency consistent with SEM observations. Such properties allowed the use of this film for the photocatalytic degradation of MR. ZnO/TiO_2 thin films have been reported for effective photocatalytic degradation of methylene blue and MR, however, it does not lead to complete mineralization [7,23,24]. In this study, ZnO thin film decolorized textile effluent by 93% with significant decrease of COD by 69%, within 3 h at room temperature. Significant degradation of ponceau 6R dye with ammonium persulfate was also achieved by photoelectrocatalytic degradation [25]. Degradation was fastest at pH 2.0 and followed first-order kinetics [26]. Our previous studies reported effective degradation of various textile dyes by *B. laterosporus, G. geotrichum,* and their consortia [20,27–29]. Results indicate that the biological treatment is more efficient than the photocatalysis-ZnO with respect to decolorization and reduction of COD. However, we cannot exclude adsorption as the experiment was conducted at pH 7, which is above the pKa (5.1) where MR is negatively charged and below the point of zero charge of ZnO (likely ˜8-9 +); and because of ionic charges present on the microbial cells. Thus removal of the dye can be attributed to both adsorption and degradation processes.

In the sequential SBAPT process (biological followed by photocatalytic treatment), resulted in 78% decolorization of MR with a 45% reduction in COD (Total treatment time: 4 h). When this sequential process was reversed (initially, photocatalysis ZnO process (2 h) followed by biological treatment (2 h)) (SPABT), decolorization increased to 100% with 80% reduction of COD (Table 1). SPABT resulted in more decolorization and reduction of COD than SBAPT and the individual treatments, since it has decreased time for the complete decolorization along with its higher degradation efficiency.

3.2. Analysis of enzymes during decolorization

The laccase induction was 750% greater in the GB consortium of SBIOT (2 h) treatment, and 2031% greater after SPABT (4 h) than in the control (0 h) (Table 2). Increased veratryl alcohol oxidase activity (45%) was observed by GB consortium of photocatalysis-ZnO treated sample (at 2 h of treatment) than control GB consortium (0 h); whereas, it was changed insignificantly in case of GB consortium without photocatalysis-ZnO treatment. Both, intracellular and extracellular tyrosinase activities were increased significantly in a GB consortium after photocatalysis-ZnO treatment (2 h) compared to the control. The analysis of reductive enzymes of GB consortium in photocatalysis-ZnO treated sample showed increased activity of azo reductase, riboflavin reductase and NADH-DCIP reductase than control (Table 2). A similar increase in enzyme activity was found in earlier reports when the GB consortium was utilized for dye degradation studies [29]. The products of photocatalysis may have induced catalytic enzymes which resulted in higher activities in the SPABT process. Induction of these enzymes was reflected in greater MR degradation within a short period.

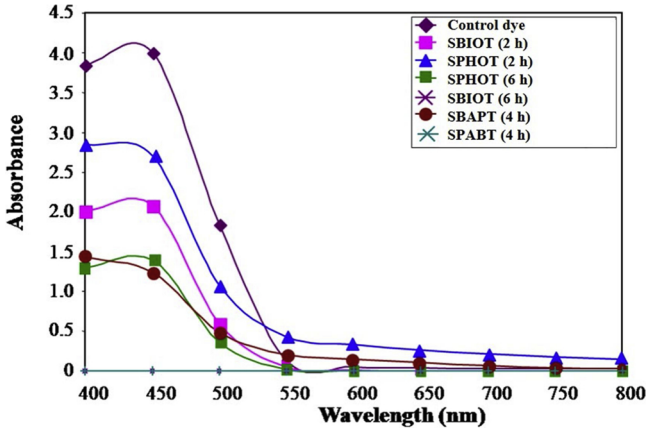

Fig. 1. UV–vis spectra of methyl red degradation by single photocatalytic treatment (2 h, 6 h), single biological treatment with GB consortium (2 h, 6 h), sequential biological and photocatalytic treatment (4 h), and sequential photocatalytic and biological treatment (4 h) (For interpretation of the references to colour in this figure legend, the reader is referred to the web version of this article).

3.3. Analysis of treatment products

3.3.1. HPTLC

Spectrophotometric examination of effluent obtained after SPHOT (2 and 6 h), SBIOT (2 and 6 h), and both the sequential processes (SBAPT and SPABT) (4 h) exhibited decrease of absorbance at 420 nm than control MR (0 h) (Fig. 1). A 2 h process with SPHOT yielded three bands on HPTLC plate (Fig. 2Bb), which increased to four bands after 6 h (Fig. 2Be), while SBIOT showed thirteen and fifteen bands after 2 and 6 h, respectively. Interestingly, SBAPT showed thirteen bands (Fig. 2Bf) in comparison with eight bands after SPABT process (4 h) (Fig. 2Bg). The differential pattern of the HPTLC chromatograms suggests greater transformation of MR in the SBAPT process.

3.3.2. HPLC

MR exhibited single major peak at 2.16 min in HPLC chromatogram (Fig. S2a). Decolorization of MR by SPHOT conducted for 2 h showed single peak at 2.47 min indicating minor biotransformation. Prolonged duration of SPHOT (6 h) suggested significant transformation of MR by showing three peaks (Fig. S2b). On the other hand, SBIOT was much more effective that showed five peaks after 2 h; while, it showed same number peaks after 6 h with changes in the retention time (Fig. S2c).

Table 2
Enzymatic analysis of control (0 h), SBIOT (2 h), SPABT (4 h) during methyl red degradation.

Enzyme		Enzyme activities of consortium GB during decolorization		
		0 h	After SBIOT	After SPABT
Laccase [a]		0.016 ± 0.02	0.120 ± 0.05*	0.325 ± 0.09*
Veratryl alcohol oxidase [a]		0.667 ± 0.08	0.725 ± 0.14	0.967 ± 0.20*
Tyrosinase [a]	Intracellular	217 ± 40	378 ± 85*	524 ± 63*
	Extracellular	239 ± 14	225 ± 74	363 ± 25*
NADH-DCIP reductase [b]		53.6 ± 0.81	68.1 ± 4.45	85.2 ± 4.52*#
Azo reductase [c]		2.95 ± 0.55	3.12 ± 0.44	4. 25 ± 0.31*
Riboflavin reductase [d]		3.70 ± 0.71	4.70 ± 0.41	6.52 ± 0.54*

[a] Enzyme activity in unit/min/mg protein.
[b] µg of DCIP reduced/min/mg protein.
[c] µM of methyl red reduced/min/mg protein.
[d] µg of riboflavin reduced/min/mg protein. Values are a mean of three experiments ± SEM. Significantly different from control (0 h) at *P < 0.05, and SBIOT at #P < 0.05 by one-way ANOVA with Tukey-Kramer comparison test.

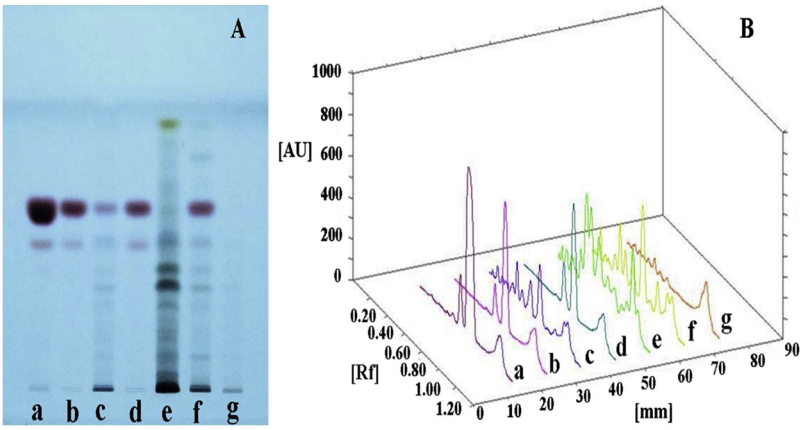

Fig. 2. (A) HPTLC profile and (B) 3-D graph; methyl red (a) and methyl red products found by the treatment of single photocatalytic treatment (2 h) (b), single biological treatment with GB consortium (2 h) (c), single photocatalytic treatment (6 h) (d), single biological treatment with GB consortium (6 h) (e), sequential biological treatment and photocatalytic treatment (4 h) (f) and sequential photocatalytic and biological treatment (4 h) (g) (For interpretation of the references to colour in this figure legend, the reader is referred to the web version of this article).

The SBAPT treatment (4 h) resulted in four peaks (Fig. S2d); whereas, SPABT (4 h) was the most efficient process among others which showed ten peaks (Fig. S2e). The peak differences in control and its formed products suggested the transformation of parent dye compound into numerous products.

3.3.3. Product characterization by FTIR

The FTIR spectrum of MR (Fig. 3) included the major peaks at 2922 cm $^{-1}$ (alkanes, C—H stretch), 1717 cm^{-1} (α-halogeno carboxylic acid, C═O stretch), 1601 cm^{-1} (azo linkage, -N═N-), 1547 cm^{-1} (N—H deformation), 1465 and 1483 cm^{-1} peaks (alkanes, $-CH_3$), 1311 cm^{-1} (C—N vibration), 1113 and 1277 cm^{-1} (alcohol, O—H deformation), and 766 and 889 cm^{-1} (C—H deformation) (Fig. 3a). A comparison of FTIR spectra of MR and its products revealed transformation MR.

After treating MR by SPHOT for 6 h, the spectrum contained all the same peaks as MR, including the azo linkage at 1604 cm^{-1}. Most importantly, this indicated that the azo bond was not cleaved during MR treatment by the photocatalytic process (Fig. 3b). Similar peaks were also observed in FTIR spectrum of the products found after 2 h of SPHOT, suggesting that there is insignificant change after 2 h of biotransformation by SPHOT (Fig. S3a).

Disappearance of the 1601 cm^{-1} peak indicates azo bond breakdown due to the azo reductase enzyme in SBIOT (Fig. 3c). The biological treatment showed a continuous change in biotransformation of parent dye molecule throughout 6 h process. There were significant changes observed during 2–6 h duration of treatment (Fig. S3b).

The difference between the FTIR spectrum of products obtained after SPABT and SBAPT was insignificant (Fig. 3d and Fig. S3c,

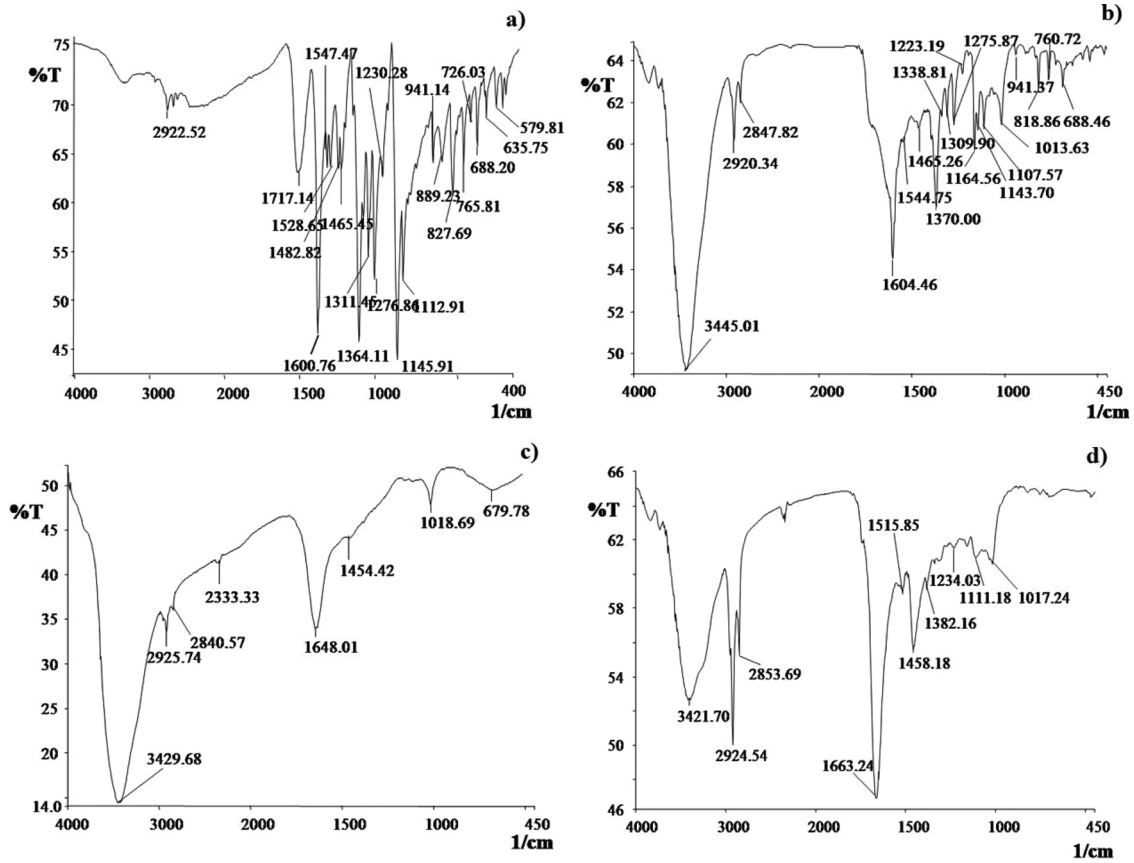

Fig. 3. FTIR spectra of methyl red (a) and methyl red products after degradation by single photocatalytic treatment (6 h) (b), single biological treatment with GB consortium (6 h) (c) and sequential photocatalytic and biological treatment (4 h) (d).

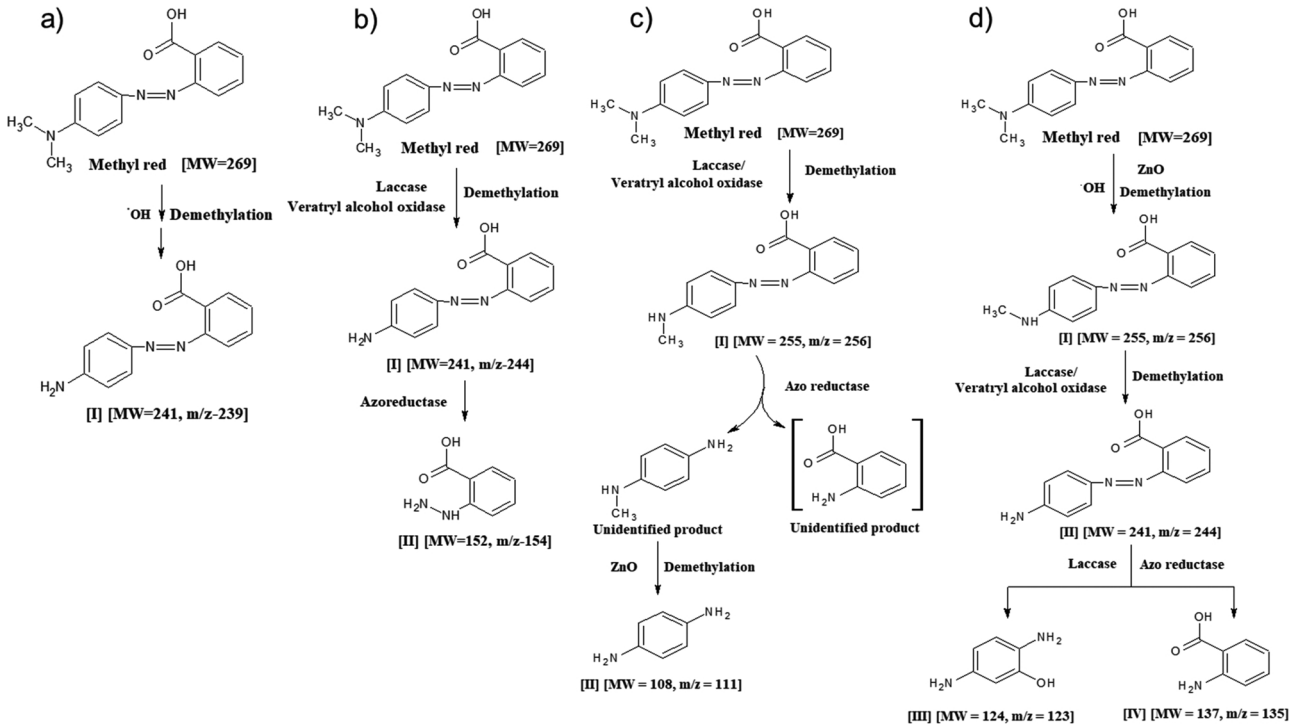

Fig. 4. Projected pathway of methyl red degradation by single photocatalytic treatment (6 h) (a) and single biological treatment with GB consortium (6 h) (b), sequential biological treatment and photocatalytic treatment (4 h) (c) and sequential photocatalytic and biological treatment (4 h) (d).

respectively). This system showed breakage of the azo bond during decolorization of MR, which led to faster and more complete degradation (Fig. 3d).

3.3.4. Degradation pathways

Fig. 4 shows proposed degradation pathways for MR after 4 h of SPHOT and SBIOT, and sequential treatments including SBAPT and SPABT after 4 h, based on MS and levels of biotransformation enzymes. The mass spectra of treatment products are provided in Table S1. In SPHOT (Fig. 4a), oxidation (demethylation) of MR was mediated by reactive oxygen species (H_2O_2, O_2, OH) that react with the dye to produce simpler products [I]. The product was identified as 2-[(4-aminophenyl) diazenyl] benzoic acid (*m/z*-239). A major finding of great importance is that the azo bond was still intact even after 6 h of SPHOT, which indicates that photocatalytic process is rapid in transformation; however, it is unable to cleave the resistant azo bonds [16]. Active oxidoreductase enzymes in the GB consortium (constituents of SBIOT) are more effective in cleaving resistant bonds, which initiated the biotransformation and biodegradation of MR (Fig. 4b). Demethylation of MR was carried out by oxidative enzyme viz., laccase/veratryl alcohol oxidase into intermediate [I], identified as 2-[(4-aminophenyl) diazenyl] benzoic acid (*m/z*-244). Induced azo reductase converted reactive intermediate 2-[(4-aminophenyl) diazenyl] benzoic acid to 2-hydrazinylbenzoic acid (*m/z*-154) (intermediate [II]).

Demethylation of MR in the SBAPT was via laccase and veratryl alcohol oxidase during first 2 h of incubation of biological treatment which yielded reactive intermediate [I], identified as 2-{[4-(methylamino)phenyl]diazenyl}benzoic acid (*m/z*-256). Biodegradation of intermediate [I] via the azo reductase enzyme generated two unidentified products. Sequential photocatalytic treatment for 2 h resulted in demethylation of one of the unidentified products to intermediate [II], identified as (1, 4-diaminobenzene (*m/z*-111) (Fig. 4c). The most desirable results were obtained when photocatalytic treatment was followed by biological treatment (SPABT) (Fig. 4d). In the SPABT, the 2-h photocatalytic process oxidized MR to 2-{[4-(methylamino)phenyl] diazenyl}benzoic acid (*m/z*-256) (intermediate [I]). This intermediate was demethylated via oxidative enzymes to 2-[(4-aminophenyl) diazenyl] benzoic acid (*m/z*-244) (intermediate [II]) during next 2 h of incubation in sequential biological treatment. Induction of azo reductase enzyme in the biological system was responsible for the further cleavage of azo linkage in intermediate [II] to produce intermediates [III] (2, 5-diaminophenol, *m/z*-123) and [IV] (2-aminobenzoic acid, *m/z*-135).

The SPABT sequential treatment was more efficient for MR degradation than the other treatments. This is likely because reaction with ROS produced during the photocatalytic stage yielded products more readily degraded by the GB consortium. Photocatalytic pretreatment has been reported to increase biodegradability of xenobiotics and reduce toxicity [12]. Photocatalytic treatment also increased biodegradability (based on an increase in the ratio of BOD/COD) of azo dyes such as reactive yellow KD-3 G, reactive red 15, reactive red 24, and cationic blue X-GRL [30]. Macroporous carriers coupling photocatalysis (TiO_2) and biodegradation (biofilm) used for degradation of reactive black 5 prevented over-oxidation and reduced the generation of toxic products [13]. The phenol and dissolved organic carbon removal efficiencies using intimately coupled visible-light-responsive photocatalysis and biodegradation in 16 h were 100% and 65%, respectively, i.e., higher than those achieved using visible-light-responsive photocatalysis (72% and 50%) or biodegradation (99% and 58%) [14].

3.4. Phytotoxicity study

Phytotoxicity tests have been used to evaluate the relative toxicity of dye effluent and treatment effectiveness [31]. Untreated MR inhibited *Phaseolus mungo* and *Sorghum vulgare* germination and reduced shoot and root lengths (Table 3). The products of SPHOT were not less phytotoxic than MR, while those resulting from SBIOT were significantly less toxic. Importantly, exposure to SPABT products showed similar growth patterns and lengths of shoot and roots similar to the control plants grown in distilled water indicating nontoxicity to the test plant species. Thus, these results confirm that SPABT system is highly efficient for rapid transformation and degradation of MR and produces

Table 3
Phytotoxicity of methyl red and its treatment products to *Phaseolus mungo* and *Sorghum vulgare*.

Sample (2000 ppm)	Plant studied					
	Phaseolus mungo			*Sorghum vulgare*		
	Germination (%)	Shoot length (cm)	Root length (cm)	Germination (%)	Shoot length (cm)	Root length (cm)
Control, distilled water	100	12.2 ± 0.3	7.6 ± 0.3	90	1.7 ± 0.1	3.5 ± 0.1
Methyl Red dye	50	6.5 ± 0.2†	2.5 ± 0.4†	20	0.4 ± 0.5†	0.3 ± 0.3†
Products of SPHOT	60	7.6 ± 0.6†	3.0 ± 0.3†	40	0.6 ± 0.9†	0.4 ± 0.4†
Products of SBIOT$^{\#}$	90	11.2 ± 0.2*	7.0 ± 0.4*	90	1.6 ± 0.6*	2.6 ± 0.8*
Products of SBAPT	70	8.0 ± 0.3*†	4.1 ± 0.1*	60	1.0 ± 0.4*†	2.3 ± 0.6*
Products of SPABT$^{\#}$	100	13.1 ± 0.1*	7.2 ± 0.6*	90	1.6 ± 0.1*	3.2 ± 0.6*

Data were subjected to a one-way ANOVA; values are means for ten germinated seeds.
† Significantly different from the seeds germinated in distilled water at $P < 0.001$.
* Significantly different from the seeds germinated in methyl red at $^{*}P < 0.01$ when analyzed by Tukey Kramer Multiple Comparison Test.
$^{\#}$ Biological treatment was with GB consortium (G- *Galactomyces geotrichum*, B-*Brevibacillus laterosporus*).

less phytotoxic products compared to the photocatalytic and biological treatments alone.

4. Conclusion

This study presents a novel method of sequential ZnO/photocatalysis and biological treatment using a microbial consortium for rapid degradation and detoxification of methyl red dye. Although a photocatalytic process alone decolorized the dye to a certain extent, it did not adequately decrease COD and phytotoxicity. This is likely because of its inability to cleave the azo bond. Photocatalytic-ZnO treatment prior to biological treatment (SPABT) enhanced decolorization rate and showed complete and rapid decolorization with the production of non-phytotoxic products. Photocatalytic treatment yields products more degradable by microbes in a sequential biological treatment. Products identified by GC–MS after the various treatments indicate different degradation pathways based on the nature and sequence of treatment.

Acknowledgments

This work was supported by the research fund of Hanyang University (HY201800000003220) to SPG. Authors (TRW) wish to thank Chinese Academy of Sciences for providing PIFI-CAS Postdoctoral Fellowship. MBK and BHJ wish to thank National Research Foundation of Korea (NRF), Ministry of Education, Science, and Technology (MEST) of the South Korean government (No. NRF-No. 2017R1A2B2004143).

Appendix A. Supplementary data

Supplementary material related to this article can be found, in the online version, at doi:https://doi.org/10.1016/j.jhazmat.2019.03.004.

References

[1] R.P. Schwarzenbach, B.I. Escher, K. Fenner, T.B. Hofstetter, C.A. Johnson, U. von Gunten, B. Wehrli, The challenge of micropollutants in aquatic systems, Science 313 (2006) 1072–1077.
[2] WHO report, Unsafe drinking-water, sanitation and waste management, Health environment and sustainable development, World Health Organization, Geneva, Switzerland, https://www.who.int/sustainable-development/cities/health-risks/water-sanitation/en/.
[3] F.M.D. Chequer, G.A.R. de Oliveira, E.R.A. Ferraz, J.C. Cardoso, M.V.B. Zanoni, D.P. de Oliveira, Textile dyes: dyeing process and environmental impact, in: M. Gunay (Ed.), Eco-Friendly Textile Dyeing and Finishing, IntechOpen Limited, London, UK, 2013, pp. 151–176.
[4] K. Santhy, P. Selvapathy, Removal of reactive dyes from wastewater by adsorption on coir pith activated carbon, Bioresour. Technol. 97 (2006) 1329–1336.
[5] C.G. Maia, A.S. Oliveira, E.M. Saggioro, J.C. Moreira, Optimization of the photocatalytic degradation of commercial azo dyes in aqueous TiO_2 suspensions, Reac. Kinet. Mech. Cat. 113 (2014) 305–320.
[6] M. Movahedi, A.R. Mahjoub, S. Janitabar-Darzi, Photodegradation of congo red in aqueous solution on ZnO as an alternative catalyst to TiO_2, J. Iran. Chem. Soc. 6 (2009) 570–577.
[7] R.T. Sapkal, S.S. Shinde, M.A. Mahadik, V.S. Mohite, T.R. Waghmode, S.P. Govindwar, K.Y. Rajpure, C.H. Bhosale, Photoelectrocatalytic decolorization and degradation of textile effluent using ZnO thin films, J. Photochem. Photobiol. B 114 (2012) 102–107.
[8] K. Kumar, S.S. Devi, K. Krishnamurthi, D. Dutta, T. Chakrabarti, Decolorisation and detoxification of direct blue-15 by a bacterial consortium, Bioresour. Technol. 98 (2007) 3168–3171.
[9] M.B. Kurade, T.R. Waghmode, J.Q. Xiong, S.P. Govindwar, B.H. Jeon, Decolorization of textile industry effluent using immobilized consortium cells in upflow fixed bed reactor, J. Clean. Prod. 213 (2019) 884–891.
[10] C.C. Oturkar, H.N. Nemade, P.M. Mulik, M.S. Patole, R.R. Hawaldar, K.R. Gawai, Mechanistic investigation of decolorization and degradation of reactive red 120 by *Bacillus lentus* BI377, Bioresour. Technol. 102 (2011) 758–764.
[11] W.Z. Tang, R. Jia, D.Q. Zhang, Decolorization and degradation of synthetic dyes by *Schizophyllum* sp. F17 in a novel system, Desalination 265 (2011) 22–27.
[12] S. Yahiat, F. Fourcade, S. Brosillon, A. Amrane, Photocatalysis as a pre-treatment prior to a biological degradation of cyproconazole, Desalination 281 (2011) 61–67.
[13] G. Li, S. Park, B.E. Rittmann, Developing an efficient TiO_2-coated biofilm carrier for intimate coupling of photocatalysis and biodegradation, Water Res. 46 (2012) 6489–6496.
[14] S. Dong, S. Dong, X. Tian, Z. Xu, D. Ma, B. Cui, N. Ren, B.E. Rittmann, Role of self-assembly coated $Er^{(3+)}$: $YAlO_3/TiO_2$ in intimate coupling of visible-light-responsive photocatalysis and biodegradation reactions, J. Hazard. Mater 302 (2016) 386–394.
[15] H.F. Xiong, D.L. Zou, D.D. Zhou, S.S. Dong, J.W. Wang, B.E. Rittmann, Enhancing degradation and mineralization of tetracycline using intimately coupled photocatalysis and biodegradation (ICPB), Chem. Eng. J. 316 (2017) 7–14.
[16] R. Comparelli, P.D. Cozzoli, M.L. Curri, A. Agostiano, G. Mascolo, G. Lovecchio, Photocatalytic degradation of methyl red by immobilised nanoparticles of TiO_2 and ZnO, Water Sci. Technol. 49 (2004) 183–188.
[17] M.N. Chong, B. Jin, C.W. Chow, C. Saint, Recent developments in photocatalytic water treatment technology: a review, Water Res. 44 (2010) 2997–3027.
[18] M.D. Marsolek, C.I. Torres, M. Hausner, B.E. Rittmann, Intimate coupling of photocatalysis and biodegradation in a photocatalytic circulating-bed biofilm reactor, Biotechnol. Bioeng. 101 (2008) 83–92.
[19] D. Chebli, F. Fourcade, S. Brosillon, S. Nacef, A. Amrane, Supported photocatalysis as a pre-treatment prior to biological degradation for the removal of some dyes from aqueous solutions; acid red 183, biebrich scarlet, methyl red sodium salt, orange II, J. Chem. Technol. Biotechnol. 85 (2010) 555–563.
[20] M.B. Kurade, T.R. Waghmode, S.M. Patil, B.H. Jeon, S.P. Govindwar, Monitoring the gradual biodegradation of dyes in a simulated textile effluent and development of a novel triple layered fixed bed reactor using a bacterium-yeast consortium, Chem. Eng. J. 307 (2017) 1026–1036.
[21] H.R. Ebrahimi, M. Modrek, Photocatalytic decomposition of methyl red dye by using nanosized zinc oxide deposited on glass beads in various pH and various atmosphere, J. Chem. 2013 (2013) 151034.
[22] S.S. Phugare, D.C. Kalyani, A.V. Patil, J.P. Jadhav, Textile dye degradation by bacterial consortium and subsequent toxicological analysis of dye and dye metabolites using cytotoxicity, genotoxicity and oxidative stress studies, J. Hazard. Mater. 186 (2011) 713–723.
[23] C. Xu, G.P. Rangaiah, X.S. Zhao, Photocatalytic degradation of methylene blue by titanium dioxide: experimental and modeling study, Ind. Eng. Chem. Res. 53 (2014) 14641–14649.
[24] F. Zhang, J. Lan, Y. Yang, T. Wei, R. Tan, W. Song, Adsorption behavior and mechanism of methyl blue on zinc oxide nanoparticles, J. Nanoparticle Res. 15 (2013) 2034–2043.
[25] A.A. El-Zomrawy, Kinetic studies of photoelectrocatalytic degradation of ponceau 6R dye with ammonium persulfate, J. Saudi Chem. Soc. 17 (2013) 397–402.
[26] K. Byrappa, A.K. Subramani, S. Ananda, K.M.L. Rai, R. Dinesh, M. Yoshimura, Photocatalytic degradation of rhodamine B dye using hydrothermally synthesized

ZnO, B. Mater. Sci. 29 (2006) 433–438.
[27] S.U. Jadhav, S.D. Kalme, S.P. Govindwar, Biodegradation of methyl red by *Galactomyces geotrichum* MTCC 1360, Int. Biodeterior. Biodegr. 62 (2008) 135–142.
[28] T.R. Waghmode, M.B. Kurade, A.N. Kabra, S.P. Govindwar, Degradation of remazol red dye by *Galactomyces geotrichum* MTCC 1360 leading to increased iron uptake in *Sorghum vulgare* and *Phaseolus mungo* from soil, Biotechnol. Bioproc. E. 17 (2012) 117–126.
[29] M.B. Kurade, T.R. Waghmode, M.U. Jadhav, B.-H. Jeon, S.P. Govindwar, Bacterial–yeast consortium as an effective biocatalyst for biodegradation of sulphonated azo dye reactive red 198, RSC Adv. 5 (2015) 23046–23056.
[30] H. Chun, W. Yizhong, Decolorization and biodegradability of photocatalytic treated azo dyes and wool textile wastewater, Chemosphere 39 (1999) 2107–2115.
[31] S.B. Jadhav, S.S. Phugare, P.S. Patil, J.P. Jadhav, Biochemical degradation pathway of textile dye remazol red and subsequent toxicological evaluation by cytotoxicity, genotoxicity and oxidative stress studies, Int. Biodeterior. Biodegr. 65 (2011) 733–743.